

RESEARCH ARTICLE

MOLECULAR DOCKING AND DRUG KINETICS ASSESSMENT FOR STRUCTURE-BASED DRUG DESIGN OF NEW PIPERAZINE-CONTAINING HYDRAZONE DERIVATIVES AS EFFECTIVE ACETYLCHOLINESTERASE INHIBITORS FOR ALZHEIMER'S DISEASE

Ibrahim Abdulganiyyu Akinbo*¹, Maimuna Shehu Rufa¹, Abduljelil Ajala², Khadija Mustapha Gwadabe¹, Aisha Yusuf Asiru³

¹Department of Public and Environmental Health, Federal University Dutse,

²Department of Chemistry, Faculty of Physical Sciences, Ahmadu Bello University, Zaria,

³Department of Biology Education, Ahmadu Bello University, Zaria, Nigeria.

Abstract

Background: Alzheimer's disease (AD), a progressive neurodegenerative disorder affecting cognitive functions, remains a critical medical challenge with limited treatment options and significant side effects. This study explores the potential of novel piperazine-containing hydrazone derivatives as acetylcholinesterase inhibitors, targeting a key enzymatic pathway implicated in AD progression. **Methods:** A structure-based drug design approach was adopted to identify and synthesize hydrazone derivatives. The study utilized the protein target 4EY7, recognized for its relevance in AD, with molecular docking and pharmacokinetic evaluations to optimize compound interaction and binding efficiency. **Results:** Fifteen hydrazone derivatives demonstrated enhanced binding interactions, stability, and superior drug-like properties compared to the reference compound. A lead compound with a binding energy of -27.23 kcal/mol showed the highest affinity and pharmacological promise, surpassing the reference compound, galantamine, in molecular docking analyses. **Conclusion:** The findings suggest that these hydrazone derivatives represent a promising class of multifunctional inhibitors with potential therapeutic applications in AD. Further investigations are warranted to validate their efficacy and safety in preclinical and clinical settings.

Keywords: Alzheimer's Disease, Computer-aided drug design, Complex mechanism, Binding energy, Pharmacokinetics

Introduction

The elderly are most affected by Alzheimer's disease (AD), a chronic neurodegenerative disorder linked to dementia and cognitive impairment (Ajala, Eltayb, et al., 2024; Borisovskaya et al., 2014; Mohamed & Rao, 2011). However, a thorough explanation of the mechanism of sickness is still pending. Numerous investigations have shown that neuro-inflammation is a significant factor in the pathophysiology of neurodegenerative disorders in the brain, which is linked to

amyloid-beta (A) deposition (Ahmad et al., 2019; Leong et al., 2020). Therefore, the inflammatory process in neurodegeneration requires that this link be broken right away (Adewale et al., 2022; Ajala et al., 2022; Behl et al., 2021; Jellinger, 2010; Kaya et al., 2016; Pathak et al., 2018).

According to recent research, molecules with the hydrazone moiety have a wide range of biological functions (Adewale et al., 2022; Ajala, Eltayb, et al., 2024; Ajala et al., 2022; Bilen et al., 2022; Kaya et al., 2016). As possible therapies for Alzheimer's disease,

pharmacologically active hydrazone derivatives with anti-neuroinflammatory properties are now being researched (Ajala et al., 2022; Kaya et al., 2016). These results led to the creation of a new class of hydrazone derivatives. With structure-based drug design, this set of investigations supports the creation of innovative and effective drugs for treating Alzheimer's disease (Adewale et al., 2022; Ajala et al., 2025; Ajala, Uzairu, et al., 2024).

Current research aims to find possible hydrazine compounds that may be used as therapeutic possibilities. Using structure-based drug design, drug properties, molecular docking, and enhanced bonding with the Human Acetylcholinesterase receptor (4EY7), which is known to complete the pertinent complex for the treatment of AD—the derivatives of hydrazone were found (Amat-Ur-Rasool & Ahmed, 2015; Marucci et al., 2021; Nadri et al., 2013; R Saxena M., 2019).

In order to better understand how and where the inhibitor binds in AD, this study aimed to perform molecular docking of hydrazone with human acetylcholinesterase to analyse the binding orientation and affinities of hydrazone.

Additionally, a lead compound that could be used to create powerful, non-toxic hydrazone derivatives with the lowest binding energy that will be assessed for pharmacokinetics and drug-likeness properties was obtained.

Materials and Procedure

Several methods have been used to identify, synthesise, and test the best hydrazone compounds that may block the Human AChE receptor (4EY7). 4EY7 is a promising target protein for the therapy of AD because of its functioning, which may prevent brain-related disorders.

Retrieval and Cleaning of Receptors

The receptor's crystallography, which was established in the literature, was gathered from the PDB (rcsb.org) and had the following features: no mutation, a lower resolution value (2.35Å), Homo sapiens, and the X-ray diffraction technique (Cheung et al., 2012). Structure validation tools known as PROCHECK have been used to discover further and verify receptor characteristics software (ebi.ac.uk/Thornton-srv/software/PROCHECK/).

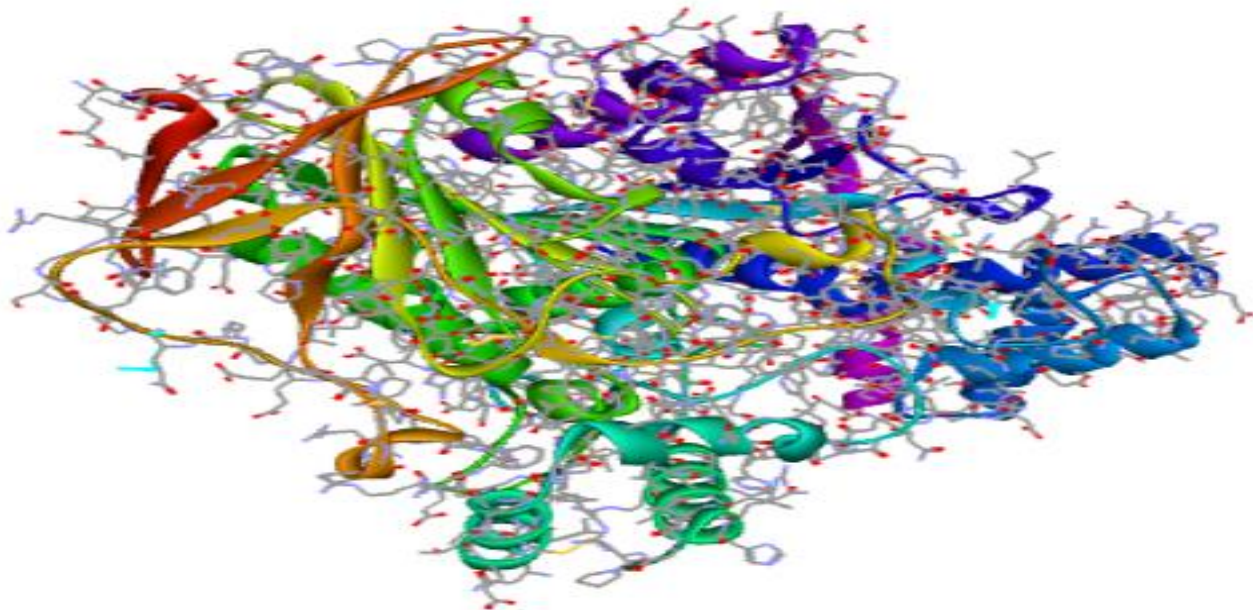


Figure 1: A cleaned and recovered receptor

Screening of Compounds

Table 1 (Kaya et al., 2016) and the binding scores for the hydrazone compounds were taken from the literature. The structures were created using ChemDraw Professional version 16.0 and saved as SD files. On the Spartan '14 interphase, it was first seen in 2D before being

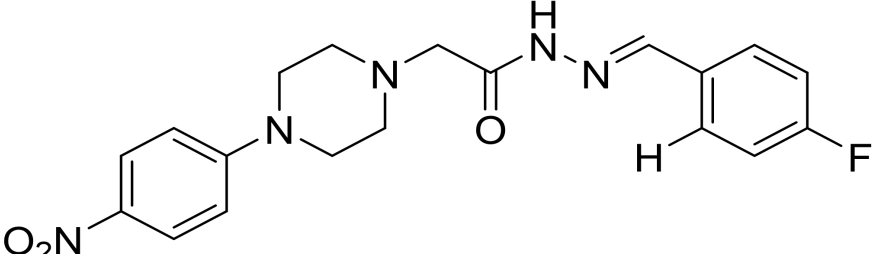
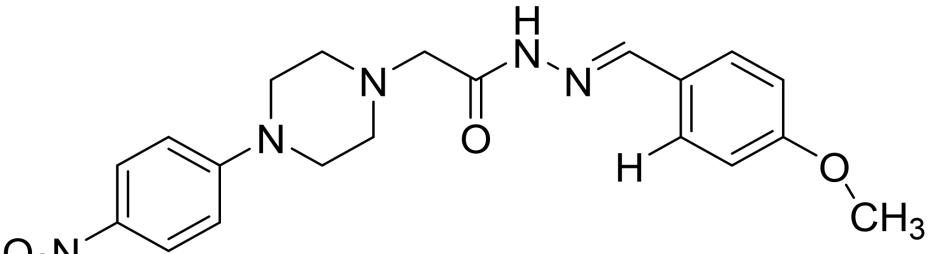
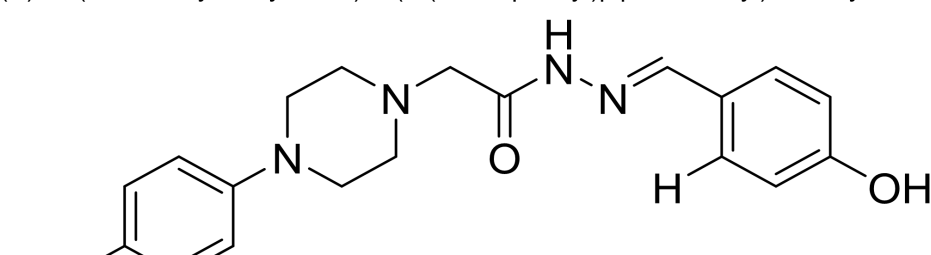
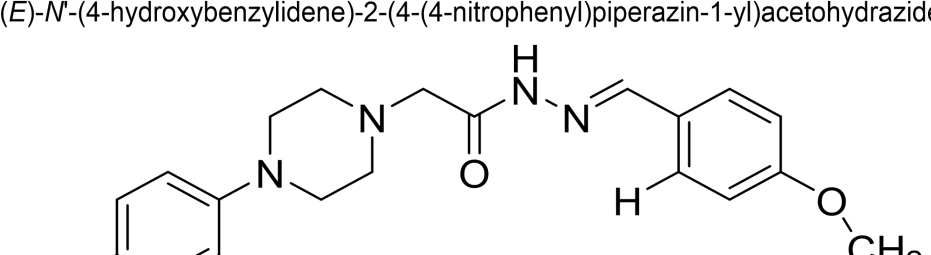
transformed to 3D. Energy minimisation was applied to the 3D molecules. Geometrical optimisation computations were carried out using a basis set of 6-31G and DFT at the B3LYP level (Ajala et al., 2022). Until they could be further examined, the chemicals were stored in a PDB file. ICM Pro, based on docking, was used to screen ligand molecules virtually (Rufa'i, Abdulganiyyu, et al., 2025).

The greatest binding interaction with the receptor, known as the binding affinity (kcal mol⁻¹), is used by ICM Pro to classify ligands (Rufa'i, Abdalla, et al., 2025) .

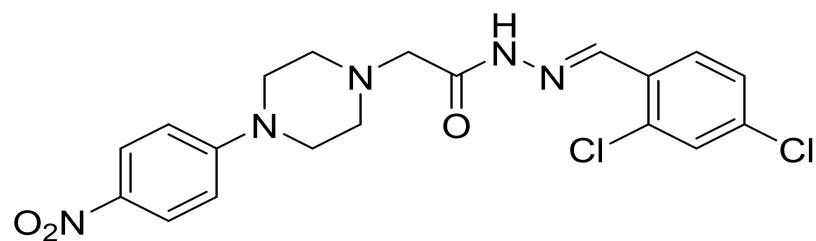
Compound Screening

For the creation of hydrazone derivatives, the molecule with the lowest scores, the strongest binding interaction, and the best stability was selected as a template (Abdulganiyyu et al., 2024; Ajala, Uzairu, et al., 2024; Akinbo et al., 2024) . The developed compounds' pharmacokinetics, drug-likeness, and physicochemical characteristics were investigated.

Table 1: Hydrazone compounds with IUPAC names and data set docking scores

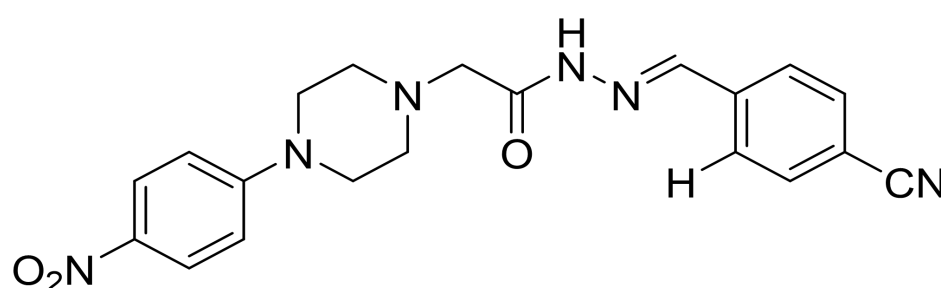
S/No	Molecule	ΔG (kcalmol ⁻¹)
1	 <i>(E)-N</i> -(4-fluorobenzylidene)-2-(4-(4-nitrophenyl)piperazin-1-yl)acetohydrazide	-20.18
2	 <i>(E)-N</i> -(4-methoxybenzylidene)-2-(4-(4-nitrophenyl)piperazin-1-yl)acetohydrazide	-15.27
3	 <i>(E)-N</i> -(4-hydroxybenzylidene)-2-(4-(4-nitrophenyl)piperazin-1-yl)acetohydrazide	-14.32
4	 <i>(E)-N</i> -(4-ethoxybenzylidene)-2-(4-(4-nitrophenyl)piperazin-1-yl)acetohydrazide	-15.44

5 -10.75



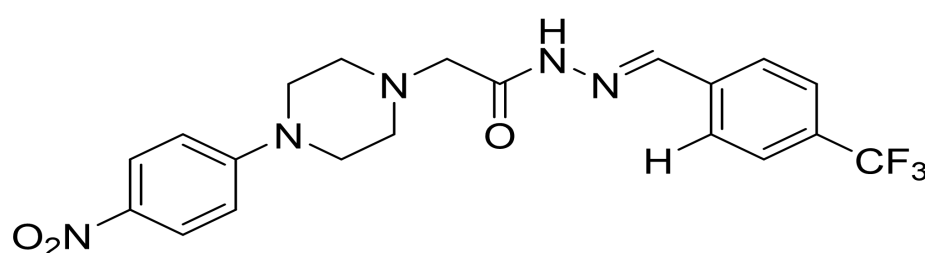
(E)-N'-(2,4-dichlorobenzylidene)-2-(4-(4-nitrophenyl)piperazin-1-yl)acetohydrazide

6 -14.87



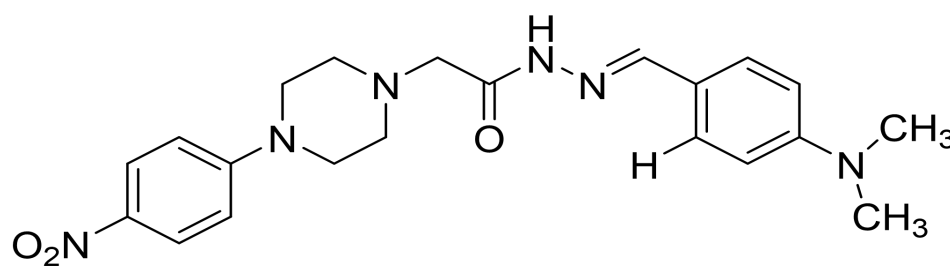
(E)-N'-(4-cyanobenzylidene)-2-(4-(4-nitrophenyl)piperazin-1-yl)acetohydrazide

7 -18.99



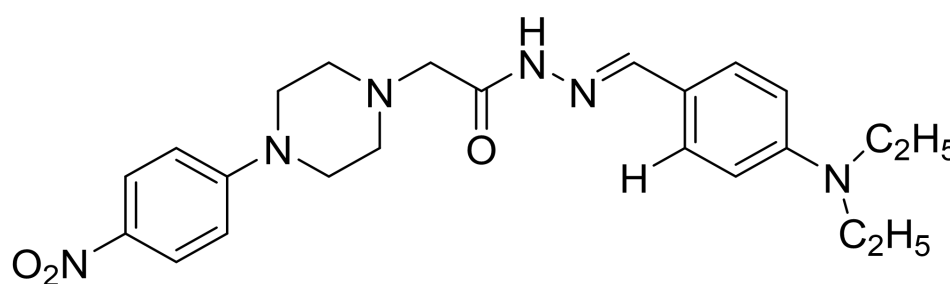
(E)-2-(4-(4-nitrophenyl)piperazin-1-yl)-N'-(4-(trifluoromethyl)benzylidene)acetohydrazide

8 -14.05

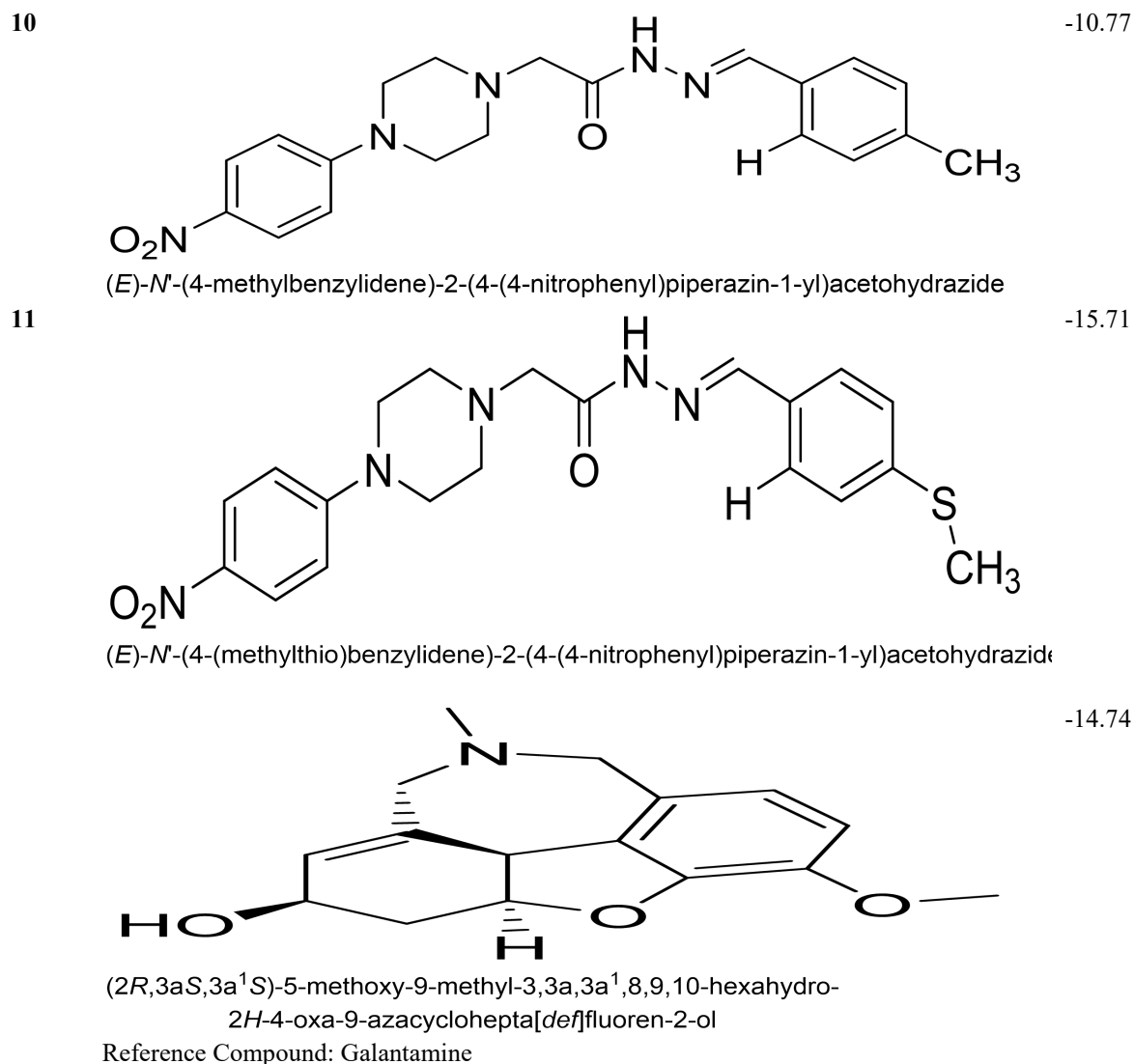


(E)-N'-(4-(dimethylamino)benzylidene)-2-(4-(4-nitrophenyl)piperazin-1-yl)acetohydrazide

9 -19.25



(E)-N'-(4-(diethylamino)benzylidene)-2-(4-(4-nitrophenyl)piperazin-1-yl)acetohydrazide



Verification, investigation of docking analysis, and validation Protocol for Docking

Every molecule in the literature was docked with the target (4EY7). The molecules with the best interaction had the lowest binding scores. Several hydrazone derivatives with better binding scores and interactions may be made using this template. The pharmacokinetic assessment and drug-like characteristics of the proposed compounds were further examined. The Glide module will be used in the Schrodinger suite to execute the docking validation methodology.

Identification and Kinetics of Drug Properties (Pharmacokinetics)

Using preadmet.qsarhub.com/ and molinspiration.com/cgi-bin/properties, the ligands'

pharmacological characteristics were determined. The hydrogen acceptor, hydrogen donor, molecular weight, number of rotatable bonds, clog P, and drug-likeness were all examined using Lipinski's Ro5. The blood-brain barrier and medication absorption in human intestines have also been studied using the Topological Polar Surface Area.

Results and Discussion

Analysis and plot of receptors

Figure 3 displays the protein target model's Ramachandran predicted plot, whose quality was evaluated using the PROCHECK online application. The model's non-glycine

and non-proline residues exhibited dihedral angles in the most preferred and additionally permitted areas. The generously permitted portions had no residue, whereas the ones that were forbidden had 0.2% residues. The optimal zone had 787 residues, and the plotted value was 90.9%. 77 residues, or 8.9% of the total, were found in the

authorised zone. Proline and glycine residue counts were 92 and 100, respectively. The Ramachandran plot showed a suitable proportion distribution of protein residues, indicating that the predicted model was of high enough quality to match the protein stereochemistry in the final model.

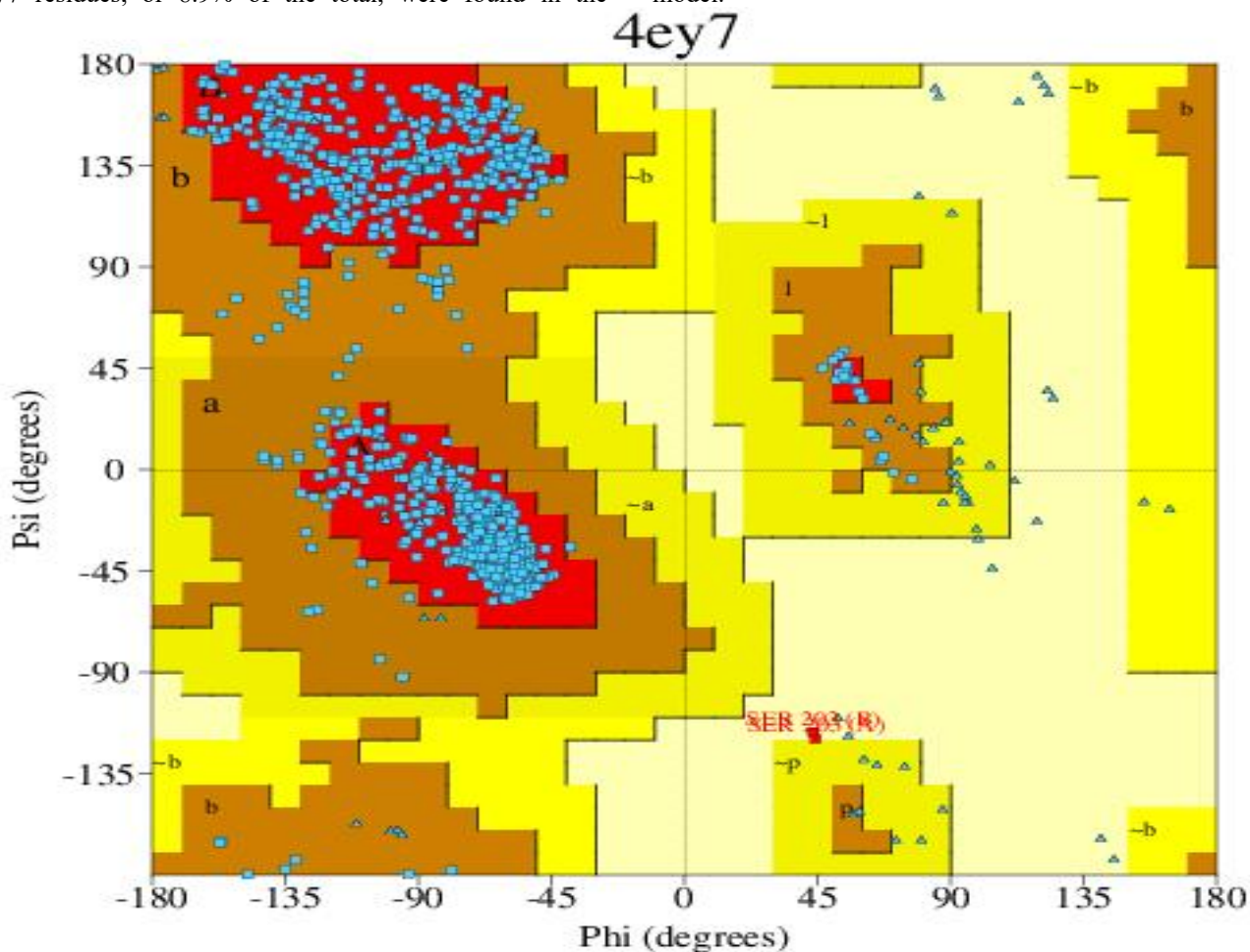


Figure 2: Ramachandran plot of Protein Target

Ligand Used for this study

most novel piperazine-containing hydrazone compounds from the literature were docked, with molecule 1 having

the lowest binding score of -20.18 kcal mol⁻¹ (See Table 1) and used as a template (Figure 3) to design several hydrazone derivatives.

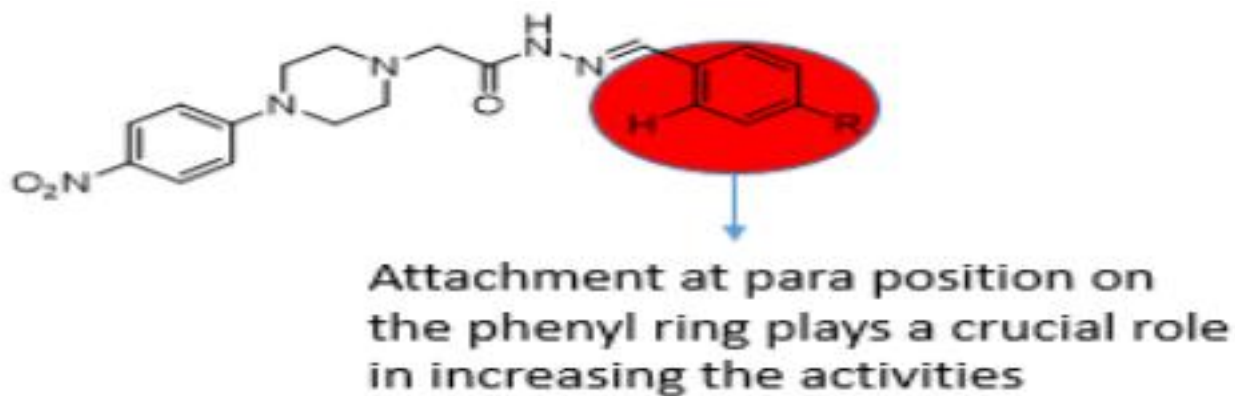


Figure 3: 2D Structure of the template compound

Verification and Inquiry of Docking Analysis and Validation Docking Protocol

The most effective way for a ligand and its receptor (therapeutic target) to interact was found using molecular docking, which helps predict molecules in a short period. As a docking process validation, the co-crystallised ligand and target from the PDB file were re-docked before the compounds were analysed to see whether the approach

was appropriate for this research specifically. According to re-docking analysis, the superimposed ligand's Root mean square deviation (RMSD), as displayed in Fig. 4 and acquired using the Schrodinger suite's Glide module, has a threshold value of $0.1943\text{\AA} < 2\text{\AA}$, demonstrating the high quality of the docking protocol and confirming the dependability of the molecular docking process (Akinbo et al., 2024).

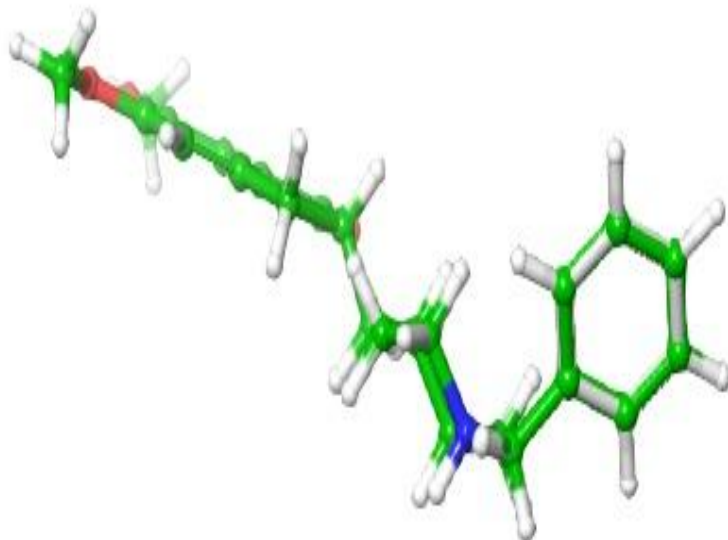
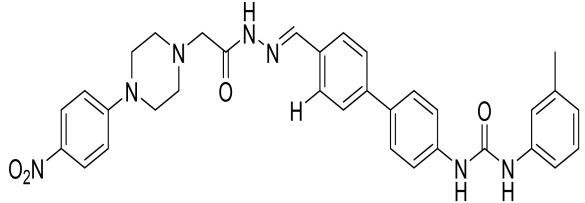
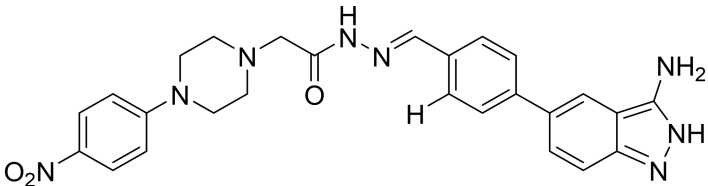
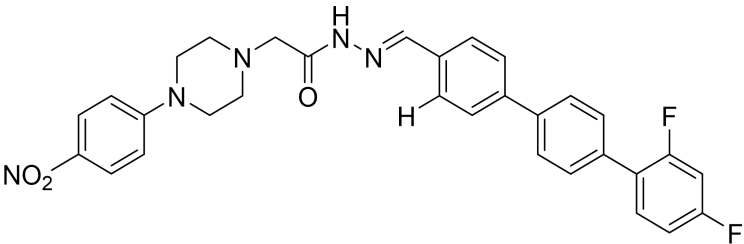
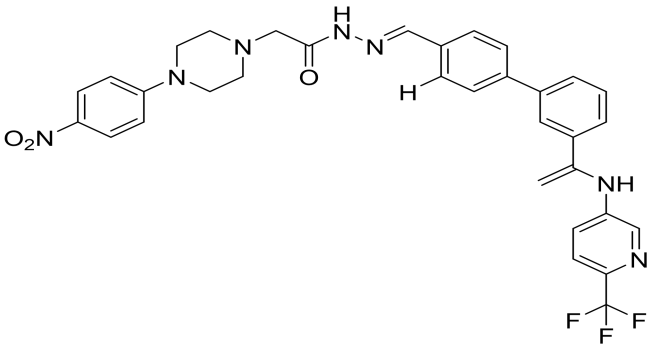


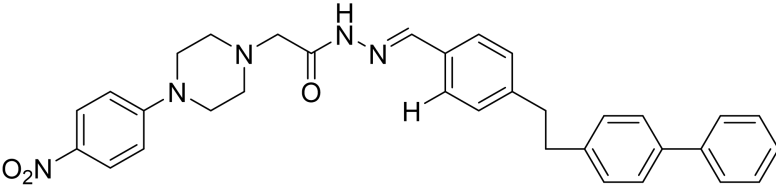
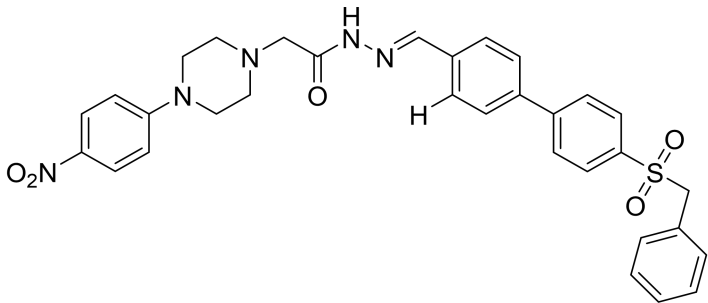
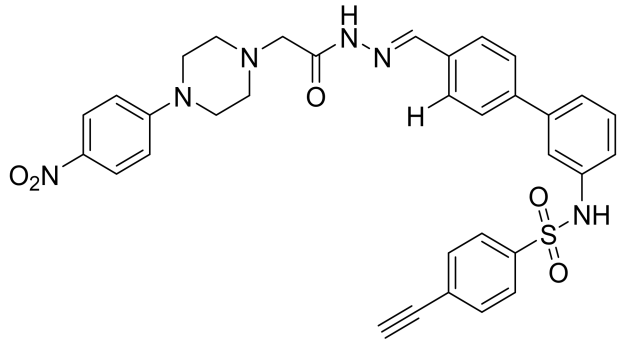
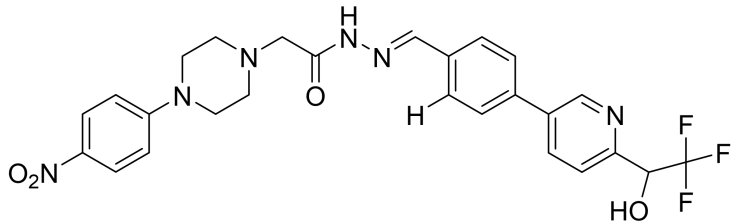
Figure 4: Superimposition of the co-crystal ligand (green) was superimposed with its docked Compound (white), revealing a significant RMSD of 0.1943 Å

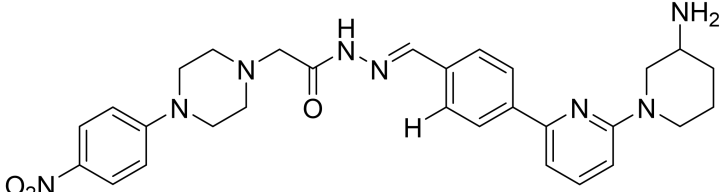
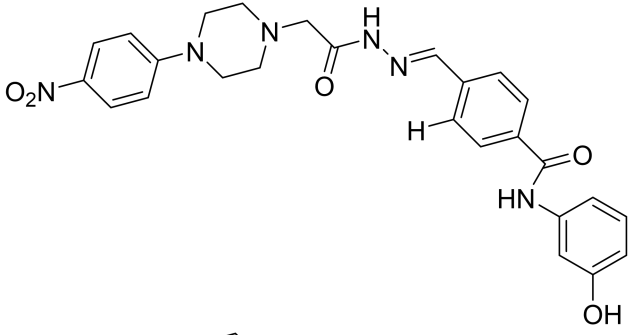
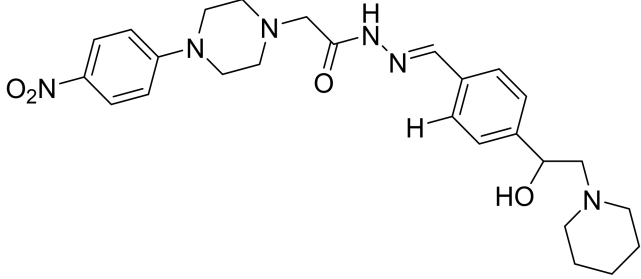
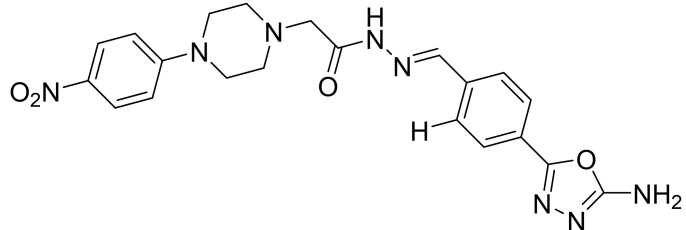
As seen in Table 2, fifteen compounds with lower binding scores and better interactions than the Template were produced by creating many hydrazone derivatives. The affinity of fifteen hydrazone derivatives for the human receptor (PDB ID: 4EY7) is shown in Table 2. Numerous linkages and the active site's highly conserved residues that bind to receptors are shown in Table 2, which supports the exceptional drugability potential of our designed compounds.

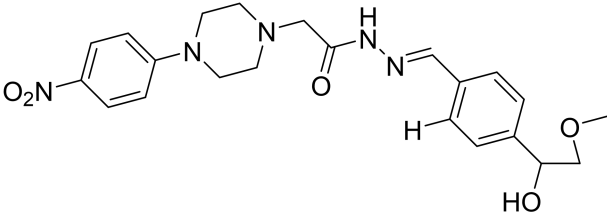
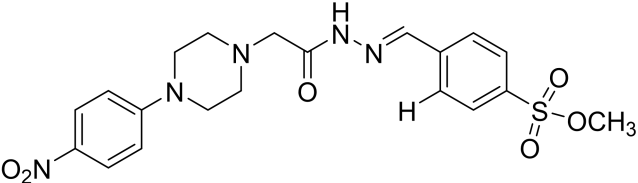
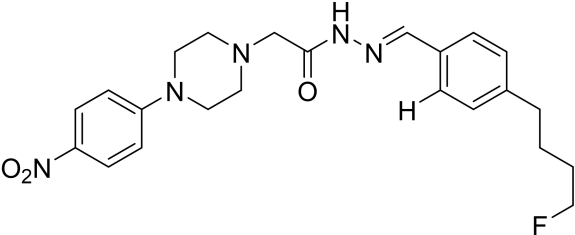
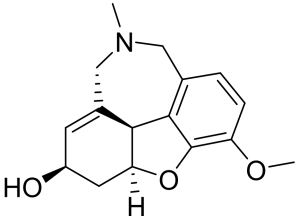
The dimensions of the docked compounds (3D and 2D) are shown in Figure 5. We can find strong inhibitors of this enzyme by molecularly docking these structures to the target's active site. The molecular docking data showed that the reference inhibitor (i.e., the Template) had higher interactions with the receptor than any developed compounds. Consequently, these compounds could block the receptors under study.

Table 2: Structures, Binding interaction of designed and reference compounds with receptor (4EY7)

S/No	ΔG (kcal mol ⁻¹)	nHB and Residue	nAmide- π Stacked and Residue	n π -Alkyl and Residue	
D1		-21.46	2 and LEU308, SER309	1 and PHE307	5 and LEU173, ALA318, HIE212, PRO216, LEU308
D2		-22.79	4 and ALA318, ASP320, ARG219, GLY220	LEU214	2 and PRO217, PRO216
D3		-22.16	1 and SER309,	2 and LEU214, PHE307	5 and MET211, ALA308, LEU315, PRO216, PRO217
D4		-23.04	2 and SER218, LEU308	2 and PHE307, LEU214	4 and LEU315, PRO216, PRO217, LEU173

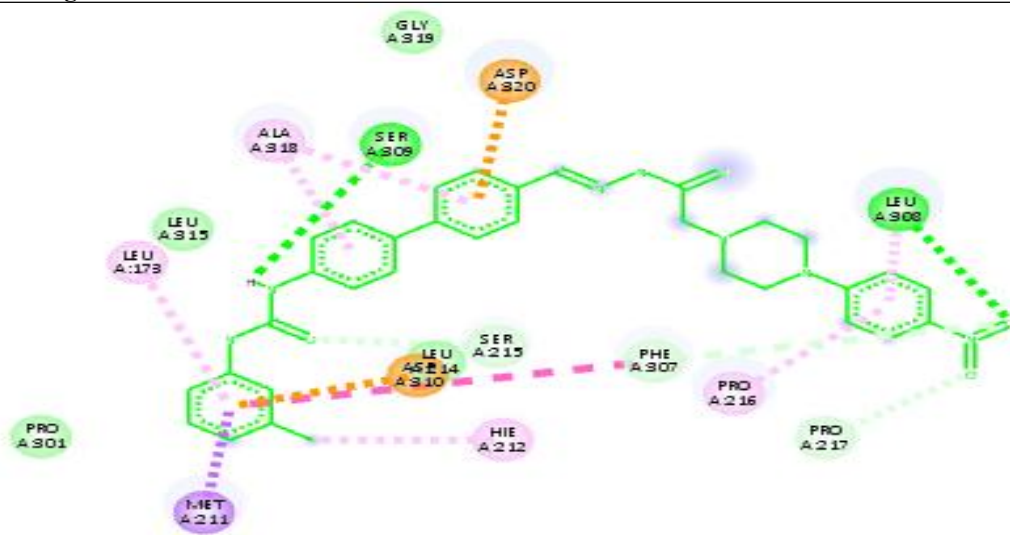
D5		-22.31	2 and LEU308, SER215	2 and SER309, PHE307	3 and ALA308, ALA314, PRO217
D6		-22.70	2 and LEU308, ASP320	2 and PHE307, LEU214	2 and ALA318, PRO216
D7		-25.93	2 and PHE307, ASP310	2 and LEU214, HIE212	5 and LEU315, ARG177, PRO217, LEU308, PRO216
D8		-27.23	3 and THR311, ASP306, ASP320	1 and SER309	1 and PRO216

D9		-21.72	1 and ALA314	1 and LEU214	2 and PRO216, PRO217
D10		-20.44	2 and LEU173, MET211	1 and LEU214	3 and PRO216, LEU315, PRO217
D11		-20.93	2 and ASP310, LEU308	1 and PHE307	3 and PRO217, LEU315, ARG177
D12		-20.22	2 and LEU308, LEU173	1 and PHE307	3 and PRO216, LEU315, PRO217

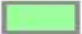

D13		-20.46	2 and LEU308, ASP310	1 and PHE307	1 and PRO217
D14		-20.81	2 and LEU308, ASN170	1 and PHE307	1 and PRO217
D15		-20.86	2 and ASP310, THR311	2 and SER309, LEU214	2 and ALA318, ALA314
REFERENCE (Galantamine)		-14.74	1 and LEU308	1 and LEU214	2 and PRO216, ALA318

S/No 2D Structures of ligand interactions

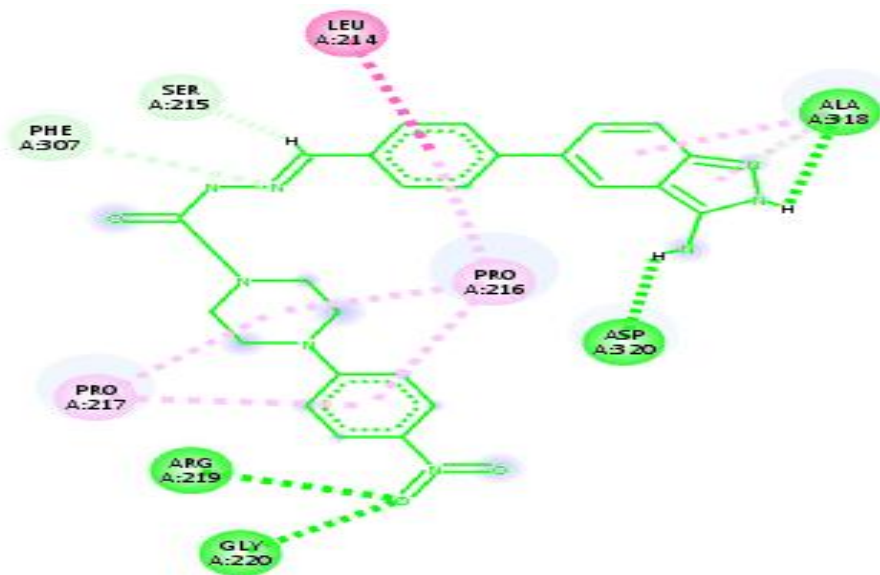
1





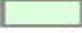


Interactions

- | | | | |
|---|----------------------------|---|------------------|
|  | van der Waals |  | Pi-Sigma |
|  | Conventional Hydrogen Bond |  | Amide-Pi Stacked |
|  | Carbon Hydrogen Bond |  | Pi-Alkyl |
|  | Pi-Anion | | |

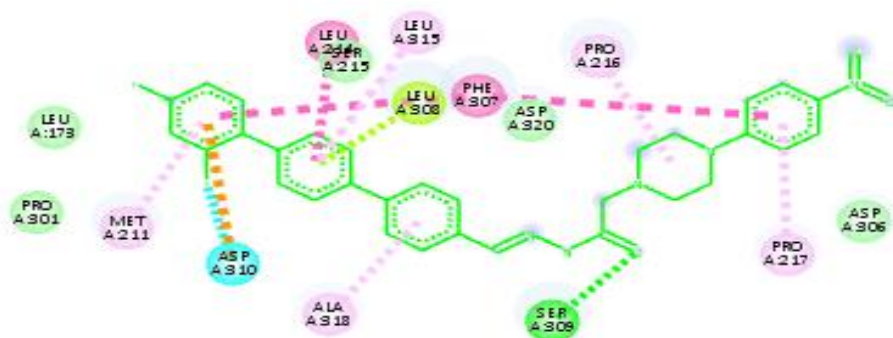
2












Interactions

- | | | | |
|---|----------------------------|---|----------|
|  | Conventional Hydrogen Bond |  | Alkyl |
|  | Carbon Hydrogen Bond |  | Pi-Alkyl |
|  | Amide-Pi Stacked | | |

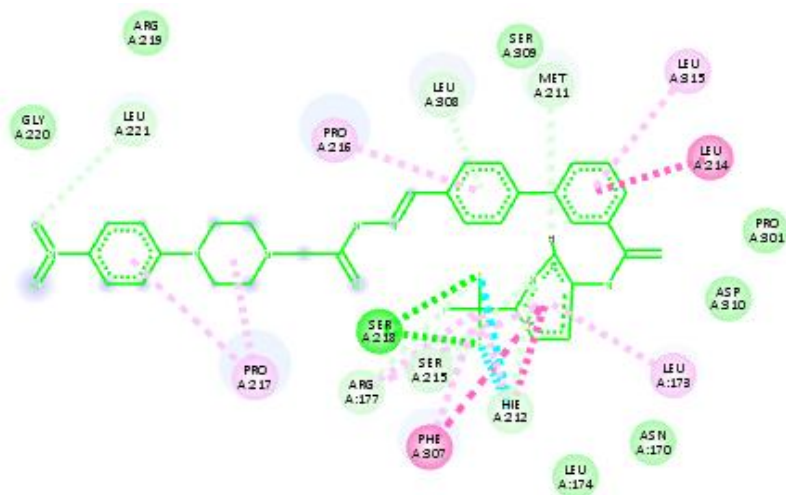
3




Interactions

- | | | | |
|---|----------------------------|---|------------------|
|  | van der Waals |  | Pi-Pi Stacked |
|  | Conventional Hydrogen Bond |  | Amide-Pi Stacked |
|  | Halogen (Fluorine) |  | Alkyl |
|  | Pi-Anion |  | Pi-Alkyl |
|  | Pi-Lone Pair | | |

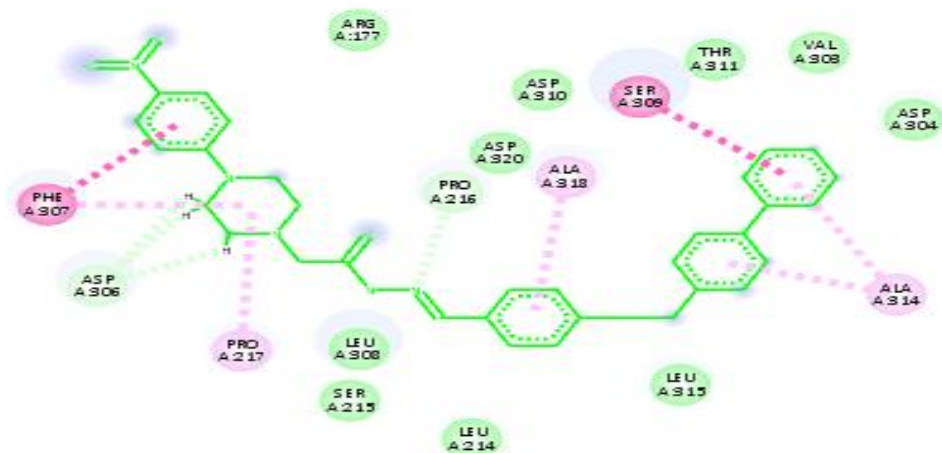
4






Interactions

- | | | | |
|---|----------------------------|---|------------------|
|  | van der Waals |  | Pi-Pi Stacked |
|  | Conventional Hydrogen Bond |  | Pi-Pi T-shaped |
|  | Carbon Hydrogen Bond |  | Amide-Pi Stacked |
|  | Halogen (Fluorine) |  | Alkyl |
|  | Pi-Donor Hydrogen Bond |  | Pi-Alkyl |

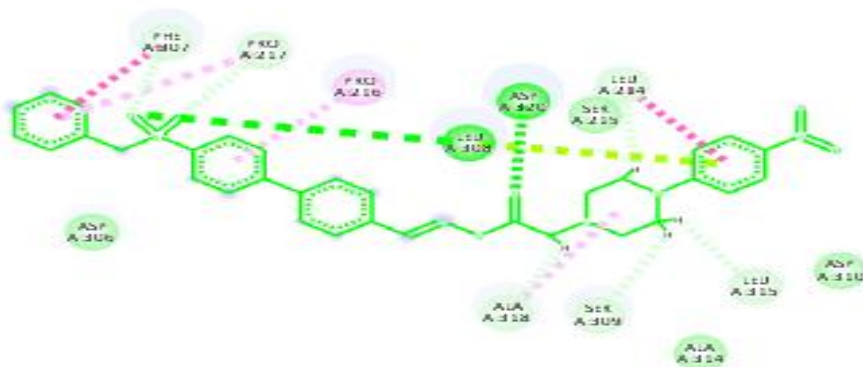
5



Interactions

- | | | | |
|---|----------------------|---|------------------|
|  | van der Waals |  | Amide-Pi Stacked |
|  | Carbon Hydrogen Bond |  | Alkyl |
|  | Pi-Pi Stacked |  | Pi-Alkyl |

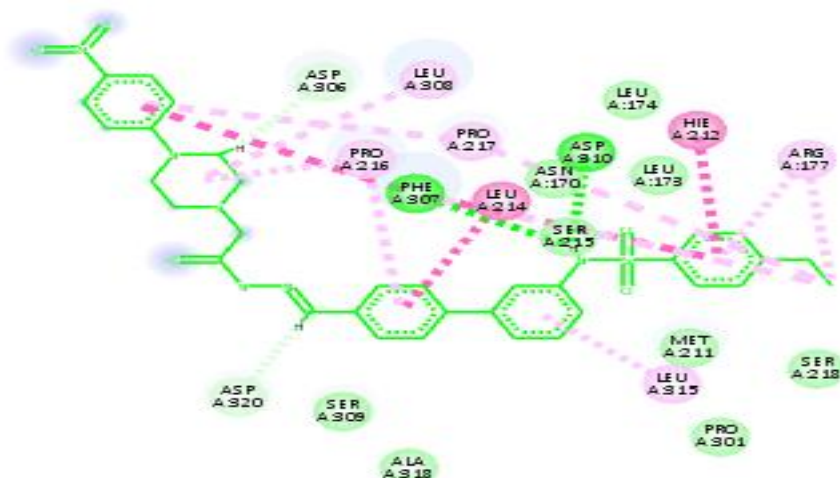
6






Interactions

- | | | | |
|---|----------------------------|---|------------------|
|  | van der Waals |  | Pi-Pi Stacked |
|  | Conventional Hydrogen Bond |  | Amide-Pi Stacked |
|  | Carbon Hydrogen Bond |  | Alkyl |
|  | Pi-Lone Pair |  | Pi-Alkyl |

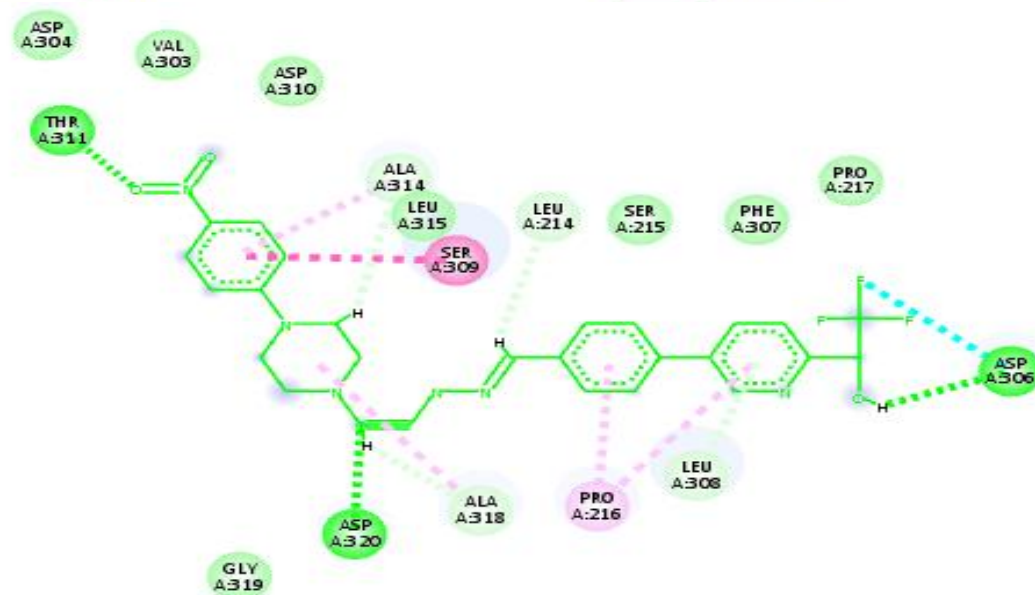
7



Interactions

- | | | | |
|---|----------------------------|---|------------------|
|  | van der Waals |  | Pi-Pi T-shaped |
|  | Conventional Hydrogen Bond |  | Amide-Pi Stacked |
|  | Carbon Hydrogen Bond |  | Alkyl |
|  | Pi-Pi Stacked |  | Pi-Alkyl |

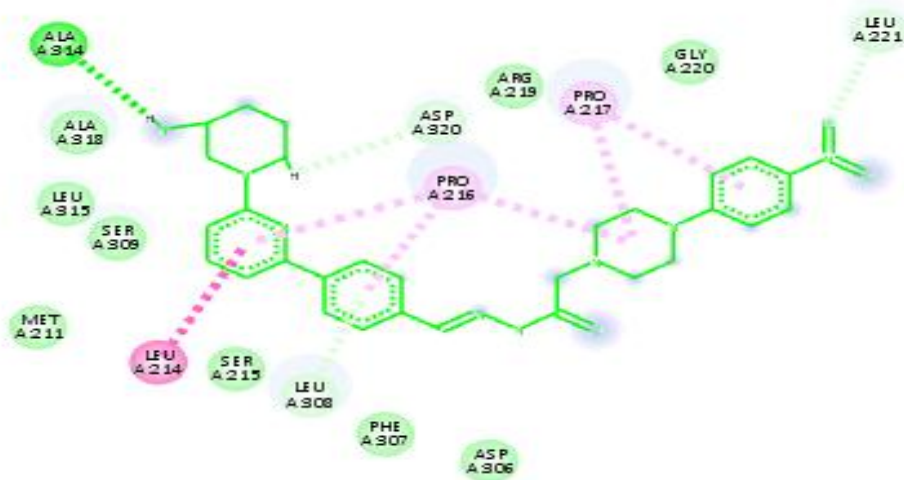
8



Interactions

- | | | | |
|---|----------------------------|--|------------------------|
|  | van der Waals |  | Pi-Donor Hydrogen Bond |
|  | Conventional Hydrogen Bond |  | Amide-Pi Stacked |
|  | Carbon Hydrogen Bond |  | Alkyl |
|  | Halogen (Fluorine) |  | Pi-Alkyl |

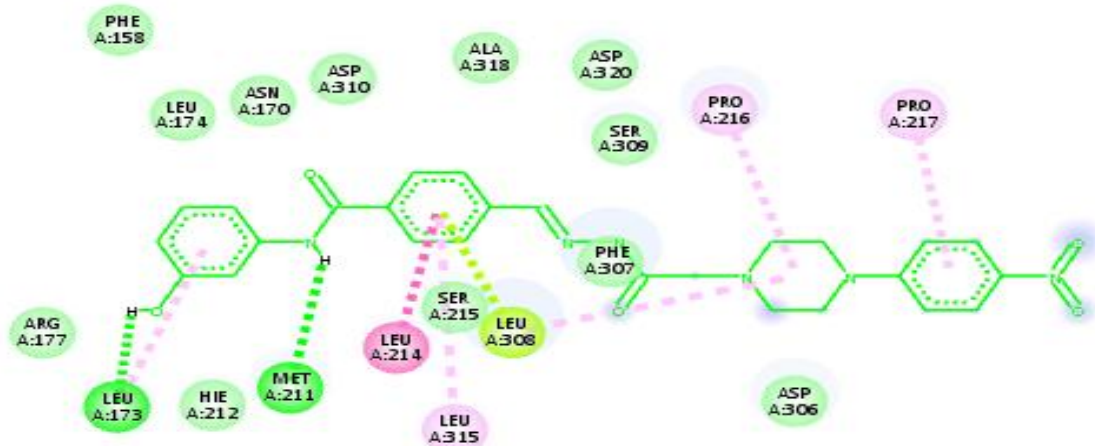
9





Interactions

- | | | | |
|---|----------------------------|--|------------------|
|  | van der Waals |  | Amide-Pi Stacked |
|  | Conventional Hydrogen Bond |  | Alkyl |
|  | Carbon Hydrogen Bond |  | Pi-Alkyl |
|  | Pi-Donor Hydrogen Bond | | |

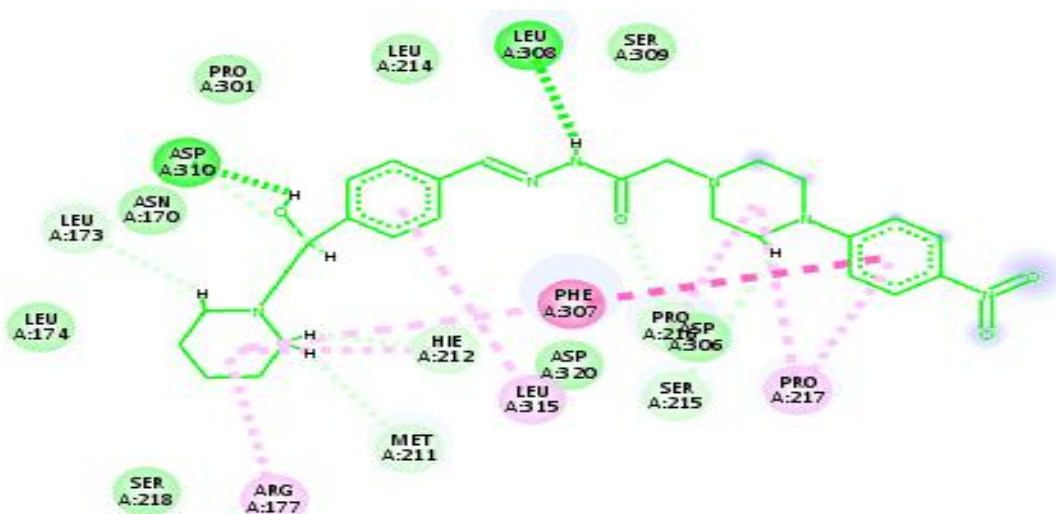
10



Interactions

- | | | | |
|---|----------------------------|--|------------------|
|  | van der Waals |  | Amide-Pi Stacked |
|  | Conventional Hydrogen Bond |  | Alkyl |
|  | Pi-Lone Pair |  | Pi-Alkyl |

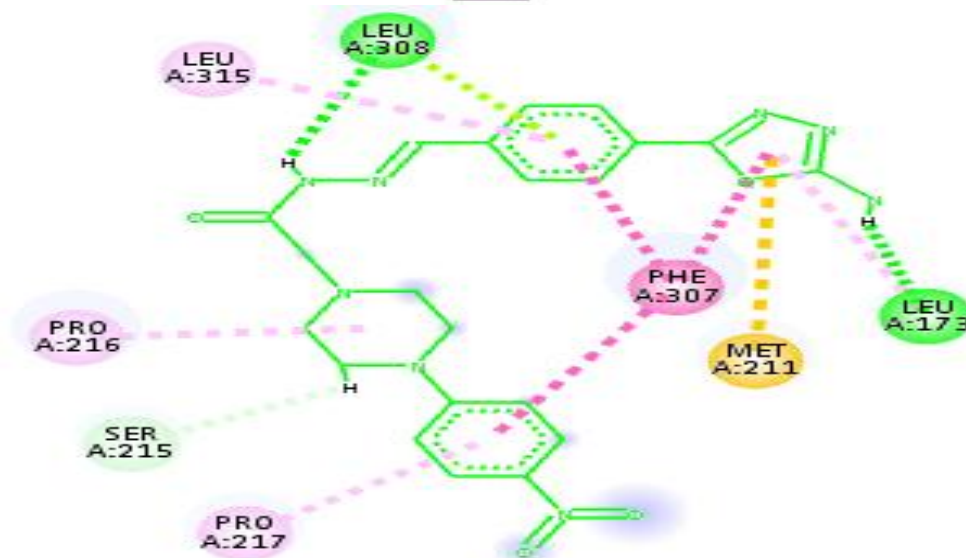
11





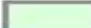





Interactions

- | | | | |
|--|----------------------------|---|---------------|
|  | van der Waals |  | Pi-Pi Stacked |
|  | Conventional Hydrogen Bond |  | Alkyl |
|  | Carbon Hydrogen Bond |  | Pi-Alkyl |

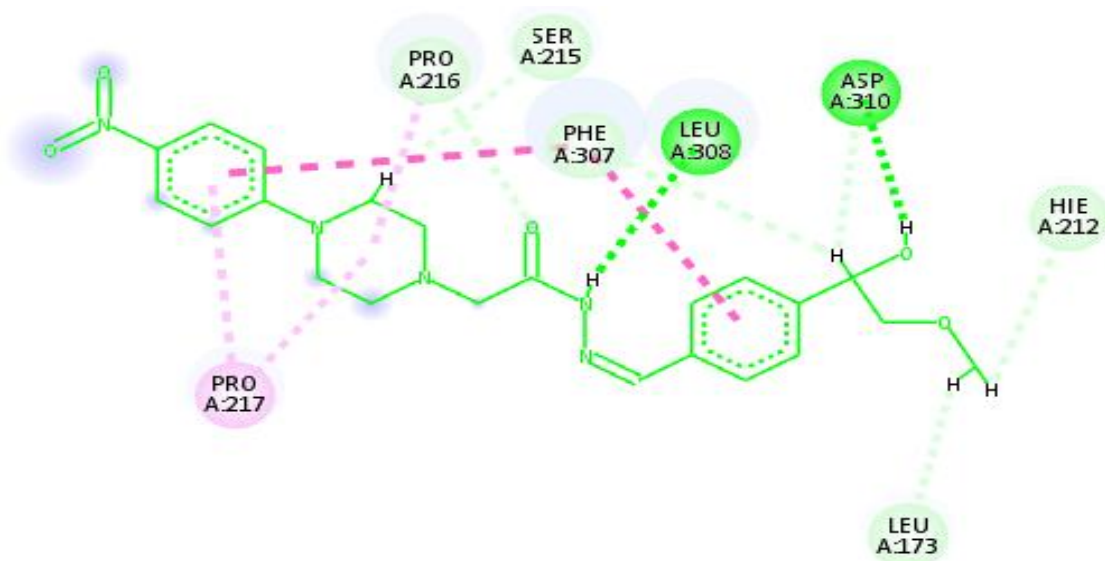
12



Interactions

- | | | | |
|---|----------------------------|---|------------------|
|  | Conventional Hydrogen Bond |  | Pi-Pi Stacked |
|  | Carbon Hydrogen Bond |  | Amide-Pi Stacked |
|  | Pi-Sulfur |  | Alkyl |
|  | Pi-Lone Pair |  | Pi-Alkyl |

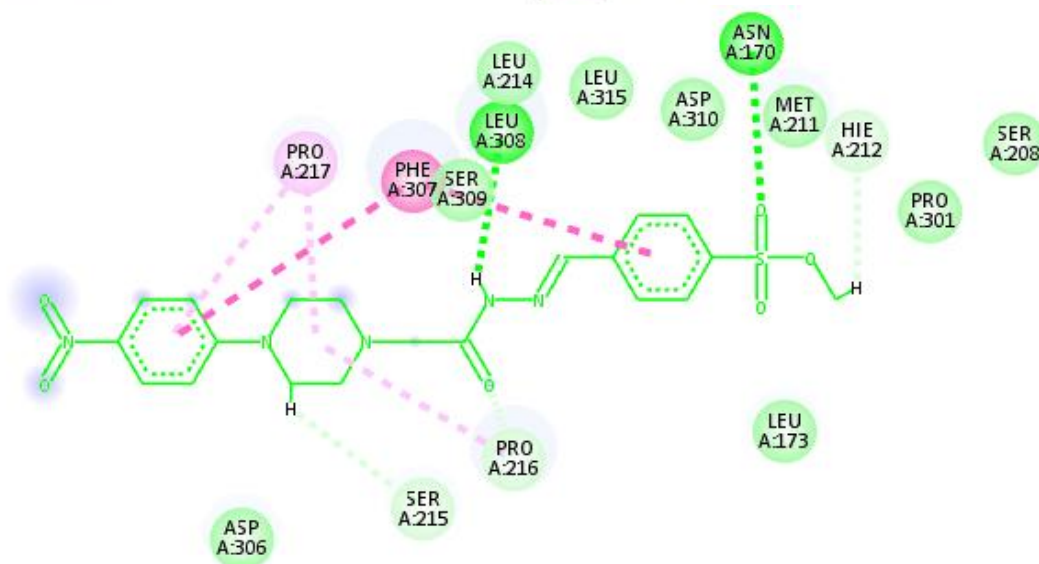
13



Interactions

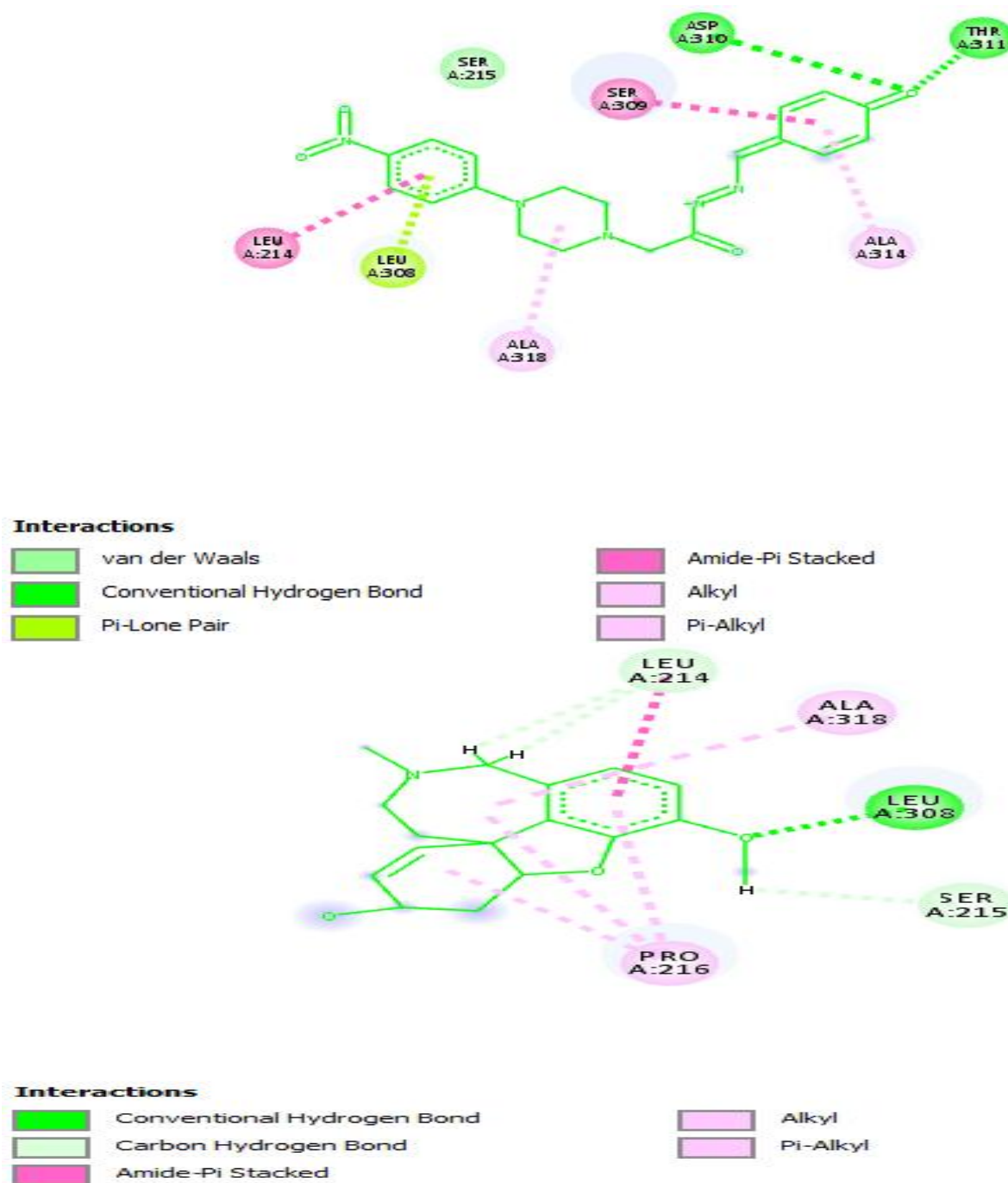
- | | | | |
|--------------------------------------|----------------------------|---------------------------------------|------------------|
| — | Conventional Hydrogen Bond | — | Amide-Pi Stacked |
| — | Carbon Hydrogen Bond | — | Alkyl |
| — | Pi-Pi Stacked | — | Pi-Alkyl |

14



Interactions

- | | | | |
|--------------------------------------|----------------------------|---------------------------------------|------------------|
| — | van der Waals | — | Amide-Pi Stacked |
| — | Conventional Hydrogen Bond | — | Alkyl |
| — | Carbon Hydrogen Bond | — | Pi-Alkyl |
| — | Pi-Pi Stacked | | |



Reference Compound Galantamine

Figure 5: 2D Visualisation of Binding Interactions of Designed Compounds and Reference Compounds

Determining the Drug's Kinetics and Properties

During drug development, the kinetics and properties of the drug are helpful for cautious and effective bonding exposure. To help determine those above, the doses of the marketed drugs were also established. Pharmacokinetic files provide professionals with pertinent data. Table 3

displays the identification of drug properties and kinetics. All of the developed compounds passed the SwissADME web server filters, and the server indicated that they were drug-like. On ascertain if the created compounds complied with Pfizer's five-point criteria, they were posted on molinspiration.com. (Daina et al., 2017)

The other four Pfizer Ro5 are included in Table 4, including (Egan et al., 2000; Middleton et al., 2005; Veber et al., 2002) , and all of the compounds that Ghose (Ghose et al., 1999; X Mahaman Y. A. R., 2019) authorised, including Teague's stringent leadlike criteria (Teague et al., 1999) . The molecules that were created showed promise as drugs. After going through the enzyme filter, compound D8 was predicted to be an AD inhibitor since it had the highest score of all the ligands, -27.23 kcal/mol. However, compound D8 established three (3) hydrogen bonds with the protein, outperforming the reference medication regarding binding affinity and

interaction. Galantamine, the reference drug employed, had a binding affinity of -14.74 kcal/mol with one (1) hydrogen bond interaction.

The likelihood that the ligand would be active increases with the score. As seen in Table 4, it was predicted that all of our drug candidates would be disease inhibitors due to the significance of this filter's prediction. According to the data shown in Table 4, none of the developed compounds broke more than two of Pfizer's rules of five (Alam & Khan, 2018; Belal, 2018; Cheng et al., 2012; Flores-Holguín et al., 2021; Moroy et al., 2012).

Table 3: Physicochemical properties of reference and designed compounds

Molecule	MW <600	Rot bonds ≤11	HBA ≤10	HBD ≤5	TPSA ≤140	Consensus Log P <5
1	591.66	12	6	3	134.89	3.63
2	498.54	8	6	3	118.46	2.25
3	555.57	9	7	1	93.76	4.68
4	629.63	7	9	2	118.68	4.65
5	547.65	8	5	1	93.76	4.58
6	597.68	9	7	1	106.28	3.7
7	522.69	9	7	2	115.31	3.45
8	542.51	10	10	2	126.88	2.74
9	542.63	9	7	2	135.91	2.11
10	494.59	10	7	2	117.23	1.85
11	400.70	8	8	3	111.9	1.94
12	450.45	8	8	2	138.7	1.06
13	441.48	10	7	2	123.22	1.11
14	445.49	9	8	1	129.12	0.83
15	461.49	9	8	1	125.51	1.23
Reference	273.33	1	4	1	41.93	1.59

Table 4: Drug-likeness analysis and reference of Designed compounds

S/No	LV	GV	VV	EV	MV	BS	PAINS	BA	SA	EI	BS
1	2	3	1	1	1	0.17	1	3	3.30	Yes	0.58
2	1	2	1	1	0	0.55	1	3	3.68	Yes	0.70
3	1	2	0	0	1	0.55	1	3	3.95	Yes	0.36
4	1	4	1	1	2	0.55	1	3	3.42	Yes	0.73
5	1	3	1	0	1	0.55	1	3	3.08	Yes	1.10
6	1	3	1	1	1	0.55	1	3	3.36	Yes	0.44
7	2	3	2	1	2	0.17	1	4	3.41	Yes	0.57
8	1	2	0	0	0	0.55	1	3	3.24	No	0.11
9	2	3	0	1	0	0.17	1	3	3.59	No	0.14
10	0	2	0	0	0	0.55	1	3	3.23	yes	0.35
11	1	0	1	1	0	0.55	1	4	3.48	Yes	0.35
12	1	0	0	1	0	0.55	1	3	3.30	Yes	0.40
13	1	0	1	0	0	0.17	1	4	3.10	Yes	0.61
14	1	0	0	0	1	0.55	1	3	3.54	Yes	0.81
15	1	0	1	0	1	0.55	1	3	3.44	Yes	0.49
Reference	0	0	0	0	0	0.55	0	1	4.07	No	-0.03

The fifteen developed compounds' predictable values for several aspects of their pharmacokinetics and pharmacological characteristics are shown in Table 5. Absorption, distribution, metabolism, excretion, and toxicity were all incorporated in the model under investigation.

Table 5 shows the suggested ligands' intestinal absorption. The pharmaceutical industry uses the in-vitro CaCo-2 device for drug development and as a model to forecast oral medication absorption. A chemical is deemed extremely permeable if its model value exceeds 70 (Fedi et al., 2021). According to the study's results, all of the produced ligands had values more than 70, which suggests that they have a high permeability towards CaCo-2 cells. A substance's degree of dispersion is determined by its distribution capacity (V), which is not the same as its physiological volume. Since a chemical is bound to bodily water, its real distribution volume cannot be more than that of physical water. The amount of free drug in plasma that may percolate and become ready to interact with the pharmacological target is the percentage of unbound drug. All of our produced compounds have VDss greater than 0.50, which indicates that the drug will be distributed throughout the tissue.

Finally, BBB penetration values reveal if a substance may cross the BBB, as seen in Table 5. In the central nervous system (CNS), a molecule is regarded as highly absorbing if its BBB value is more than 2.0 and as having intermediate absorption if its value is between 2.0 and 0.1 (Neumaier et al., 2021).

A chemical or its metabolite(s) is mostly eliminated from the body by metabolism and excretion. The findings indicated that the proposed compounds had modest absorption to the central nervous system. Substance metabolism is the chemical or enzymatic transformation of the parent substance into one or more readily excretable metabolites, with renal or biliary clearance being the main excretion route. According to Table 5, none of our compounds are substrates of the renal organic cation transporter 2 (total clearance) (OCT2), and all have excellent renal elimination (0.5–8.4 mL/min/kg). Lastly, toxicity testing verified the safety of every chemical created. Lastly, Table 5 demonstrates that any compound has the potential to be a useful drug.

Conclusion

This research developed hydrazone analogues, which were shown to be acetylcholinesterase inhibitors for Alzheimer's disease, using structure-based drug design. These methods provide crucial direction for creating new, powerful hydrazone derivatives with reduced Gibbs free energy (kcal/mol). With a docking score of -20.18 kcal mol⁻¹, the lead Compound (also known as the Template) emerged victorious as the molecule with the greatest interaction and stability. Fifteen new Alzheimer's inhibitors with improved interactions, docking scores, drug-likeness, and drug kinetics were therefore designed using it. With the most powerful Compound, 8, scoring 27.23 kcal mol⁻¹ with the 4EY7 receptor, the docking study revealed significant active site residues involved in the binding interactions of all the suggested compounds. It demonstrated the dependability and safety of the created compounds.

An Abbreviations List

Alzheimer's disease, or AD SA: Accessibility Synthetic, BS: Bioavailability Score, BA: Brenk alerts, The following infractions are listed: GV: Ghose, LV: Lipinski, EV: Egan, VV: Veber, and MV: Muegge. HIA: Absorption via the human gut, BBB: penetration of the blood-brain barrier, Enzyme Inhibitor (EI) and Bioactivity Score (BS).

Table 5: Pharmacokinetic and toxicity analysis of designed and reference compounds

	Models	1	2	3	4	5	6	7	8	9	10	11	12	13	14	15	Reference
Absorption	A	0.60	0.74	0.68	0.51	0.83	0.74	1.18	0.96	0.53	0.72	0.64	0.95	0.37	0.06	0.24	1.37
	B	86.33	89.21	88.96	91.92	90.01	88.85	82.41	80.54	81.37	93.24	97.75	90.22	73.99	72.29	67.94	94.38
	C	-3.74	-2.74	-2.85	-2.74	-2.66	-2.74	-3.94	-2.77	-2.78	-2.80	-3.88	-2.77	-2.74	-2.74	-2.85	-3.03
Distribution	D	0.71	0.71	0.65	0.59	0.58	0.92	1.35	0.54	0.90	1.12	0.50	0.55	0.59	0.58	0.01	0.71
	E	0.24	0.34	0.22	0.37	0.21	0.23	0.15	0.12	0.15	0.32	0.33	0.17	0.39	0.07	0.24	0.58
	F	0.71	1.21	0.60	1.11	0.17	0.75	0.79	1.05	0.67	0.646	0.748	1.107	-0.94	-0.90	-1.02	0.25
	G	-1.08	-1.83	-1.99	-1.11	-1.07	-1.44	-1.51	-1.55	-1.64	-2.98	-1.89	-1.61	-3.00	-3.15	-3.16	-2.81
Metabolism	H	Yes	Yes	No	No	No	No	No	No	No	Yes	No	No	No	No	No	Yes
	I	Yes	Yes	Yes	Yes	Yes	Yes	Yes	Yes	Yes	Yes	Yes	Yes	Yes	Yes	Yes	No
	J	Yes	Yes	No	No	No	No	No	No	No	No	No	No	No	No	No	Yes
	K	Yes	Yes	Yes	Yes	No	Yes	Yes	Yes	Yes	No	No	No	No	No	No	Yes
	L	Yes	Yes	No	Yes	No	No	Yes	Yes	No	No	No	No	Yes	No	No	Yes
	M	Yes	Yes	No	No	No	No	No	Yes	No	Yes	No	No	No	No	No	Yes
N	Yes	Yes	Yes	Yes	Yes	Yes	Yes	Yes	Yes	Yes	Yes	No	Yes	Yes	Yes	Yes	No
Excretion	O	0.57	0.71	0.62	0.87	0.54	0.88	0.92	1.76	0.67	1.67	0.81	1.52	0.17	0.42	0.45	0.15
	P	No	No	No	No	No	No	No	No	No	No	No	No	No	No	No	Yes
Toxicity	Q	No	No	No	No	No	No	No	No	No	No	No	No	No	No	No	Yes
	R	No	No	No	No	No	No	No	No	No	No	No	No	No	No	No	Yes
	T	No	No	No	No	No	No	No	No	No	No	No	No	No	No	No	Yes

A; CaCO₃ (log Papp in 10⁻⁶ cm/s), B; Human Intestinal Absorption (% Absorbed), C; Skin permeability (log Kp), D; VD_{ss} (human) (log L/kg), E; Fraction unbound (human) (Fu), F; BBB permeability (log BB), G; CNS permeability (log PS), H; CYP2D6 substrate, I; CYP3A4 substrate, J; CYP1A2 inhibitor, K; CYP2C19 inhibitor, L; CYP2C9 inhibitor, M; CYP2D6 inhibitor, N; CYP3A4 inhibitor, O; Total clearance (log ml/min/kg), P; Renal OCT2 substrate (Yes/No), Q; AMEX toxicity (Yes/No), R; Human ether-a-go-go-related gene inhibition, S; Carcinogens (mol/kg), T; Hepatotoxicity

Acknowledgement

We wish to acknowledge the Department of Public and environmental Health and the Faculty of Basic Medical Sciences Drug design laboratory

Source of Funding: None

Conflict of interest: The authors declare that they have no competing interests

Authors' contribution:

AAI: Conceptualization, Computational works and manuscript writing, MSR: Conceptualization, Manuscript writing and editing, AA: Computational works and conceptualization, KMG: manuscript writing and AYA: manuscript writing and editing .

Article History:

Received:26th November, 2024.

Accepted: 22nd February 2025.

Published online: 3rd October 2025

REFERENCES

- Abdulganiyyu, I. A., Ajala, A., Rufai, M. S., Babalola, B. J., Ufeli, B. S., Adamu, L. H., Abbas, N., Ahmad, I. S., Usman, J. D., Aujara, K. M., & Sambo, A. (2024). An Evaluation of the Pharmacokinetics and Virtual Screening of Highly Effective Hybrid Compounds for Alzheimer's Disease. *Journal of Environmental Bioremediation and Toxicology*, 7(2), 63–74. <https://doi.org/10.54987/JEBAT.V7I2.1046>
- Adewale, B. S., Igie, N., & Odeyemi, I. (2022). Structure-based discovery of multi-target directed anti-inflammatory p-nitrophenyl hydrazones; molecular docking, drug-likeness, in-silico pharmacokinetics, and toxicity studies. In *ChemRxiv* (Vol. 3). <https://doi.org/10.26434/chemrxiv-2022-mrptw>
- Ahmad, S. S., Khan, H., Rizvi, S. M. D., Ansari, S. A., Ullah, R., Rastrelli, L., Mahmood, H. M., & Siddiqui, M. H. (2019). Computational study of natural compounds for the clearance of amyloid-beta: A potential therapeutic management strategy for Alzheimer's disease. *Molecules*, 24(18), 1–11. <https://doi.org/10.3390/molecules24183233>
- Ajala, A., Asipita, O. H., Michael, A. T., Tajudeen, M. T., Abdulganiyyu, I. A., & Ramu, R. (2025). Therapeutic exploration potential of adenosine receptor antagonists through pharmacophore ligand-based modelling and pharmacokinetics studies against Parkinson disease. *In Silico Pharmacology*, 13, 17. <https://doi.org/10.1007/s40203-025-00305-9>
- Ajala, A., Eltayb, W. A., Abatyough, T. M., Ejeh, S., El fadili, M., Otaru, H. A., Edache, E. I., Abdulganiyyu, A. I., Areguamen, O. I., Patil, S. M., & Ramu, R. (2024). In-silico screening and ADMET evaluation of therapeutic MAO-B inhibitors against Parkinson disease. *Intelligent Pharmacy*, 2(4). <https://doi.org/10.1016/j.ipha.2023.12.008>
- Ajala, A., Uzairu, A., Shallangwa, G. A., & Abechi, S. E. (2022). Structure-Based Drug Design of Novel Piperazine Containing Hydrazone Derivatives as Potent Alzheimer Inhibitors: Molecular Docking and Drug Kinetics Evaluation. *Brain Disorders*, 7(June), 100041. <https://doi.org/10.1016/j.dscb.2022.100041>
- Ajala, A., Uzairu, A., Shallangwa, G. A., Abechi, S. E., Umar, A. B., Abdulganiyyu, I. A., Ramu, R., & Kumar, N. (2024). QSAR application of natural therapeutics inhibitors against Alzheimer's disease through in-silico virtual-screening, docking-simulation, molecular dynamics, and pharmacokinetic prediction analysis. *Intelligent Pharmacy*, 2(4), 505–515. <https://doi.org/10.1016/J.IPHA.2023.12.004>
- Akinbo, I. A., Ajala, A., Rufai, M. S., Baiwa, F. I., Kurawa, M. M., Jackson, G. E., Ismaila, S. S., Babalola, B. J., Ufeli, B. S., Adamu, L. H., Mustapha, A., Yahaya, N., Abba, J. E., Hussaini, H., Kazaure, M. B., & Garba, A. (2024). Theoretical examination of molecular docking, pharmacokinetics and in-silico design of specific tacrine derivatives as anti-Alzheimer agents. *Dutse Journal of Pure and Applied Sciences*, 10, 187–201. <https://doi.org/10.4314/dujopas.v10i3a.18>
- Alam, S., & Khan, F. (2018). QSAR, docking, ADMET, and system pharmacology studies on tormentic acid derivatives for anticancer activity. *Journal of Biomolecular Structure and Dynamics*, 36(9), 2373–2390. <https://doi.org/10.1080/07391102.2017.1355846>
- Amat-Ur-Rasool, H., & Ahmed, M. (2015). Designing second generation anti-Alzheimer compounds as inhibitors of Human acetylcholinesterase: Computational screening of synthetic molecules and dietary phytochemicals. *PLoS ONE*, 10(9). <https://doi.org/10.1371/journal.pone.0136509>
- Behl, T., Makkar, R., Sehgal, A., Singh, S., Sharma, N., Zengin, G., Bungau, S., Andronie-Cioara, F. L., Munteanu, M. A., Brisc, M. C., Uivarosan, D., & Brisc, C. (2021). Current trends in neurodegeneration: Cross talks between oxidative stress, cell death, and inflammation. *International Journal of Molecular Sciences*, 22(14). <https://doi.org/10.3390/ijms22147432>
- Belal, A. (2018). Drug likeness, targets, molecular docking and ADMET studies for some indolizine derivatives. *Pharmazie*, 73(11), 635–642. <https://doi.org/10.1691/ph.2018.8061>
- Bilen, E., Özmen, Ü. Ö., Çete, S., Alyar, S., & Yaşar, A. (2022). Bioactive sulfonyl hydrazones with alkyl derivative: Characterization, ADME properties, molecular docking studies and investigation of inhibition on choline esterase enzymes for the diagnosis of Alzheimer's disease. *Chemico-Biological Interactions*, 360(April), 109956. <https://doi.org/10.1016/j.cbi.2022.109956>
- Borisovskaya, A., Pascualy, M., & Borson, S. (2014). Cognitive and Neuropsychiatric Impairments in Alzheimer's Disease: Current Treatment Strategies. *Current Psychiatry Reports*, 16(9). <https://doi.org/10.1007/s11920-014-0470-z>

- Cheng, F., Li, W., Zhou, Y., Shen, J., Wu, Z., Liu, G., Lee, P. W., & Tang, Y. (2012). admetSAR: A Comprehensive Source and Free Tool for Assessment of Chemical ADMET Properties. *Journal of Chemical Information and Modeling*, 52(11), 3099–3105. <https://doi.org/10.1021/ci300367a>
- Cheung, J., Rudolph, M. J., Burshteyn, F., Cassidy, M. S., Gary, E. N., Love, J., Franklin, M. C., & Height, J. J. (2012). Structures of Human Acetylcholinesterase in Complex with Pharmacologically Important Ligands. <https://doi.org/10.1021/jm300871x>
- Daina, A., Michielin, O., & Zoete, V. (2017). SwissADME: A free web tool to evaluate pharmacokinetics, drug-likeness and medicinal chemistry friendliness of small molecules. *Scientific Reports*, 7(January), 1–13. <https://doi.org/10.1038/srep42717>
- Egan, W. J., Merz, K. M., & Baldwin, J. J. (2000). Prediction of drug absorption using multivariate statistics. *Journal of Medicinal Chemistry*, 43(21), 3867–3877. <https://doi.org/10.1021/jm000292e>
- Fedi, A., Vitale, C., Ponschin, G., Aychunie, S., Fato, M., & Scaglione, S. (2021). In vitro models replicating the human intestinal epithelium for absorption and metabolism studies: A systematic review. In *Journal of Controlled Release* (Vol. 335). <https://doi.org/10.1016/j.jconrel.2021.05.028>
- Flores-Holguín, N., Frau, J., & Glossman-Mitnik, D. (2021). Computational Pharmacokinetics Report, ADMET Study and Conceptual DFT-Based Estimation of the Chemical Reactivity Properties of Marine Cyclopeptides. *ChemistryOpen*, 10(11), 1142–1149. <https://doi.org/10.1002/open.202100178>
- Ghose, A. K., Viswanadhan, V. N., & Wendoloski, J. J. (1999). A knowledge-based approach in designing combinatorial or medicinal chemistry libraries for drug discovery. 1. A qualitative and quantitative characterization of known drug databases. *Journal of Combinatorial Chemistry*, 1(1), 55–68. <https://doi.org/10.1021/cc9800071>
- Jellinger, K. A. (2010). Basic mechanisms of neurodegeneration: A critical update. *Journal of Cellular and Molecular Medicine*, 14(3). <https://doi.org/10.1111/j.1582-4934.2010.01010.x>
- Kaya, B., Özkay, Y., Temel, H. E., As, Z., & Kaplanc, J. (2016). Synthesis and Biological Evaluation of Novel Piperazine Containing Hydrazone Derivatives. *Journal of Chemistry*, 2016, 1–8. <https://doi.org/10.1155/2016/5878410>
- Leong, Y. Q., Ng, K. Y., Chye, S. M., Pick, A., Ling, K., & Koh, R. Y. (2020). Mechanisms of action of amyloid-beta and its precursor protein in neuronal cell death. *Metabolic Brain Disease*, 35, 11–30.
- Marucci, G., Buccioni, M., Ben, D. D., Lambertucci, C., Volpini, R., & Amenta, F. (2021). Efficacy of acetylcholinesterase inhibitors in Alzheimer's disease. *Neuropharmacology*, 190, 108352. <https://doi.org/10.1016/j.neuropharm.2020.108352>
- Middleton, P., Stewart, F., Al-Qahtani, S., Egan, P., O'roure, C., Abdulrahman, A., Byres, M., Middleton, M., Kumarasamy, Y., Shoeb, M., Nahar, L., Delazar, A., & Sarker, S. D. (2005). Antioxidant, antibacterial activities and general toxicity of alnus glutinosa, fraxinus excelsior and papaver rhoeas. *Iranian Journal of Pharmaceutical Research*, 4(2). <https://doi.org/10.22037/IJPR.2010.620>
- Mohamed, T., & Rao, P. P. N. (2011). Alzheimer's Disease: Emerging Trends in Small Molecule Therapies. *Current Medicinal Chemistry*, 18(28), 4299–4320. <https://doi.org/10.2174/092986711797200435>
- Moroy, G., Martiny, V. Y., Vayer, P., Villoutreix, B. O., & Miteva, M. A. (2012). Toward in silico structure-based ADMET prediction in drug discovery. *Drug Discovery Today*, 17(1–2), 44–55. <https://doi.org/10.1016/j.drudis.2011.10.023>
- Nadri, H., Pirali-Hamedani, M., Moradi, A., Sakhteman, A., Vahidi, A., Sheibani, V., Asadipour, A., Hosseinzadeh, N., Abdollahi, M., Shafiee, A., & Foroumadi, A. (2013). 5,6-Dimethoxybenzofuran-3-one derivatives: A novel series of dual Acetylcholinesterase/Butyrylcholinesterase inhibitors bearing benzyl pyridinium moiety. *DARU, Journal of Pharmaceutical Sciences*, 21(1). <https://doi.org/10.1186/2008-2231-21-15>
- Neumaier, F., Zlatopolskiy, B. D., & Neumaier, B. (2021). Drug penetration into the central nervous system: Pharmacokinetic concepts and in vitro model systems. In *Pharmaceutics* (Vol. 13, Issue 10). <https://doi.org/10.3390/pharmaceutics13101542>
- Pathak, A., Rohilla, A., Gupta, T., Akhtar, M. J., Haider, M. R., Sharma, K., Haider, K., & Yar, M. S. (2018). DYRK1A kinase inhibition with emphasis on neurodegeneration: A comprehensive evolution story-cum-perspective. *European Journal of Medicinal Chemistry*, 158, 559–592. <https://doi.org/10.1016/j.ejmech.2018.08.093>
- R Saxena M., & D. (2019). Target enzyme in Alzheimer's disease: Acetylcholinesterase inhibitors. *Current Topics in Medicinal Chemistry*, 19(4), 264–275. <https://doi.org/10.1002/ijch.201900130>
- Rufa'i, M. S., Abdalla, M., Abdulganiyyu, I. A., Ajala, A., Alahmadi, R. M., Awadalla, M. E., Abdulganiyyu, K., Mahe, A., Gwarzo, Y. S., & Kabir, N. (2025). In-silico design of 3-Methyl-3H-naphtho[1,2,3-de]quinoline-2,7-dione Inhibitors against Tuberculosis via Docking and Dynamics Simulation Techniques, and Pharmacokinetic Evaluation. *ASPET Discovery*, 100007. <https://doi.org/10.1016/J.ASPETD.2025.100007>
- Rufa'i, M. S., Abdulganiyyu, I. A., Ajala, A., Abdalla, M., Alahmadi, R. M., Awadalla, M. E., Abdulganiyyu, K., Mahe, A., Gwarzo, Y. S., & Kabir, N. (2025). In-silico design and evaluation of quinoline-dione derivatives as Mycobacterium tuberculosis DprE1 inhibitors. *Discover Molecules* 2025 2:1, 2(1), 1–15. <https://doi.org/10.1007/S44345-025-00027-7>
- Teague, S. J., Davis, A. M., Leeson, P. D., & Oprea, T. (1999). The design of leadlike combinatorial libraries. *Angewandte Chemie - International Edition*, 38(24), 3743–3748. [https://doi.org/10.1002/\(SICI\)1521-3773\(19991216\)38:24<3743::AID-ANIE3743>3.0.CO;2-U](https://doi.org/10.1002/(SICI)1521-3773(19991216)38:24<3743::AID-ANIE3743>3.0.CO;2-U)
- Veber, D. F., Johnson, S. R., Cheng, H. Y., Smith, B. R., Ward, K. W., & Kopple, K. D. (2002). Molecular properties that influence the oral bioavailability of drug candidates. *Journal of Medicinal Chemistry*, 45(12), 2615–2623. <https://doi.org/10.1021/jm020017n>
- X Mahaman Y. A. R., H. F. K. A. H. M. T. M. S. G. B. & W. (2019). Involvement of calpain in the neuropathogenesis of Alzheimer's disease. *Medicinal Research Reviews*, 39(2), 608–630. <https://doi.org/10.1002/med.21534>